DSP-based Robust Nonlinear Speed Control of PM Synchronous Motor

In-Cheol Baik, Kyeong-Hwa Kim and Myung-Joong Youn

Abstract

A DSP-based robust nonlinear speed control of a permanent magnet synchronous motor(PMSM) is presented. A quasi-linearized and decoupled model including the influence of parameter variations and speed measurement error on the nonlinear speed control of a PMSM is derived. Based on this model, a boundary layer integral sliding mode controller to improve the robustness and performance of the nonlinear speed control of a PMSM is designed and compared with the conventional controller. To show the validity of the proposed control scheme, simulations and experimental works are carried out and compared with the conventional control scheme.

I. Introduction

PMSM drives are being increasingly used in a wide range of applications due to their high power density, large torque to inertia ratio, and high efficiency. This paper deals with the nonlinear speed control of a surface mounted permanent magnet synchronous motor with sinusoidal flux distribution. Since the dynamics of the currents is much faster than that of the mechanical speed, the speed is considered as a constant parameter rather than a state variable and they can be approximately linearized by the field orientation and current control [1-4]. However, for low power servo drives, this approximate linearization leads to the lack of torque due to the incomplete current control during the speed transient and reduces the control performance [5-6].

A solution to overcome this problem proposed by Le Pioufle [7] is to consider the motor speed as a state variable in electrical equations, which results in a nonlinear model. Then the nonlinear control method, so called feedback linearization technique, is applied to obtain an exactly linearized and decoupled model and the linear design technique is employed to complete the control design [8]. Since the nonlinear controller is very sensitive to the speed measurement error, even small error of speed measurement results in a significant speed error and its robustness can be improved by carefully selecting the control gains in the linear control loops [7]. However, besides the speed measurement error, there are parameter variations such as the stator resistance, flux, and inertia due to the temperature rise and load variations. The stator resistance and flux variations also show a steady state error and the inertia and flux variations degrade transient performance. The steady state error may also go to zero by properly choosing the linear controller gains. However, the transient performance can still be significantly degraded due to the inertia and flux variations.

The feedback linearization deals with the technique of transforming the original system model into an equivalent model of a simpler form, and then employs the well-known and powerful linear design technique to complete the control design. However, it does not guarantee the robustness in the presence of parameter uncertainties or disturbances and the drawbacks of the conventional nonlinear control scheme result from this fact. To overcome these drawbacks, we consider the feedback linearization technique as a model-simplifying device for the robust control [9]. Therefore, in this paper, a quasi-linearized and decoupled model including the influence of parameter variations and speed measurement error on the nonlinear speed control of a PMSM is firstly derived and then the robust control scheme employing a boundary layer integral sliding mode is designed to improve the control performance for both the transient and steady state.

II. Nonlinear Speed Control of PMSM Using Input-Output Linearization

1. Modeling of PMSM

The machine considered is a surface mounted PMSM and

Manuscript received February 18, 1997; accepted December 8, 1997.

The authors are with the Department of Electrical Engineering, Korea Advanced Institute of Science and Technology.

the nonlinear state equation in the synchronous dq reference frame can be represented as follows :

$$\frac{dx}{dt} = f(x) + Gu \tag{1}$$

where

$$x = \begin{pmatrix} x_1 \\ x_2 \\ x_3 \end{pmatrix} = \begin{pmatrix} i_d \\ i_q \\ \Omega \end{pmatrix} \tag{2}$$

$$u = \begin{pmatrix} u_1 \\ u_2 \end{pmatrix} = \begin{pmatrix} v_d \\ v_q \end{pmatrix} \tag{3}$$

$$G = \begin{pmatrix} \frac{1}{L_d} & 0 \\ 0 & \frac{1}{L_q} \\ 0 & 0 \end{pmatrix} \tag{4}$$

$$f(x) = \begin{pmatrix} f_1(x) \\ f_2(x) \\ f_3(x) \end{pmatrix} = \begin{pmatrix} -\frac{R}{L_d} x_1 + P\frac{L_q}{L_d} x_2 x_3 \\ -P\frac{L_d}{L_q} x_1 x_3 - \frac{R}{L_q} x_2 - P\frac{\Phi}{L_q} x_3 \\ P\frac{3}{2}\frac{\Phi}{J} x_2 - \frac{F}{J} x_3 - \frac{T_L}{J} \end{pmatrix}. \tag{5}$$

The variables and parameters used in these equations are defined as follows :

- v_d, v_q : stator voltages in the direct and quadrature axes
- i_d, L_q : current and inductance in the direct axis
- i_q, L_q : current and inductance in the quadrature axis
- R : stator resistance
- Ω : mechanical speed of motor
- P : number of pole pairs
- Φ : flux linkage created by the rotor magnets
- J : moment of inertia
- F : viscous friction coefficient
- T_L : load torque
- f_1, f_2, f_3 : nonlinear terms in a PMSM model.

2. Nonlinear Speed Control of PMSM

In order to get a total input-output linearization, the direct axis current and mechanical speed are chosen as outputs. From eq.(1) and the assumption that the load torque is considered to be an unknown constant, differentiation of the output is taken until the direct relationship between the outputs and inputs of the model can be obtained as follows [7-9] :

$$\begin{pmatrix} \frac{di_d}{dt} \\ \frac{d^2\Omega}{dt^2} \end{pmatrix} = B + A \begin{pmatrix} v_d \\ v_q \end{pmatrix} \tag{6}$$

where

$$B = \begin{pmatrix} f_1 \\ \frac{3}{2}\frac{1}{J}\left\{P\Phi f_2 - \frac{2}{3}Ff_3\right\} \end{pmatrix} \tag{7}$$

$$A = \begin{pmatrix} \frac{1}{L_d} & 0 \\ 0 & \frac{3P\Phi}{2L_qJ} \end{pmatrix}. \tag{8}$$

Because the order of eq.(1) is same as that of eq.(6), there is no internal dynamics. The nonlinear control input which permits a linearized and decoupled behavior is deduced from this relationship as follows :

$$\begin{pmatrix} v_d \\ v_q \end{pmatrix} = A^{-1}\left(-B + \begin{pmatrix} \nu_1 \\ \nu_2 \end{pmatrix}\right) \tag{9}$$

where ν_1 and ν_2 are the new control inputs. By Substituting eq.(9) into (6), the linearized and decoupled model can be given as

$$\frac{di_d}{dt} = \nu_1 \tag{10}$$

$$\frac{d^2\Omega}{dt^2} = \nu_2. \tag{11}$$

As the control laws for the new control inputs, the linear controller suggested by Le Pioufle becomes as follows [7] :

$$\nu_1 = K_{11}(i_d^* - i_d) \tag{12}$$

$$\nu_2 = \frac{d^2\Omega^*}{dt^2} + K_{21}\frac{d}{dt}(\Omega^* - \Omega) + K_{22}(\Omega^* - \Omega). \tag{13}$$

where K_{11}, K_{21}, and K_{22} are the gains. Also, i_d^* and Ω^* are the tracking commands of the direct axis current and mechanical speed of a PMSM, respectively. As a result, the following error dynamics can be obtained as

$$\frac{de_1}{dt} + K_{11}e_1 = 0 \tag{14}$$

$$\frac{d^2e_2}{dt^2} + K_{21}\frac{de_2}{dt} + K_{22}e_2 = 0 \tag{15}$$

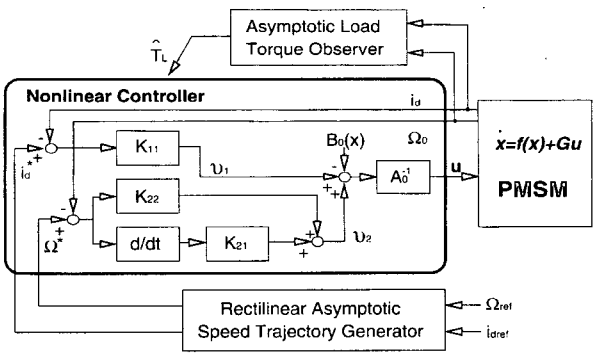

Fig. 1. Block diagram of the conventional nonlinear control scheme.

where $e_1 = i_d^* - i_d$, $e_2 = \Omega^* - \Omega$. The poles for the desired error dynamics can be chosen by properly selecting the gains using a binomial standard form, etc. [10]. The overall scheme of

the conventional nonlinear speed control system is shown in Fig. 1. As shown in this figure, by employing a rectilinear asymptotic speed trajectory generator, the acceleration command is within the maximum permissible value of a motor. As a result, the quadrature axis current can be made not exceed its maximum permissible value [7].

3. Asymptotic Load Torque Observer

For the control scheme proposed in this paper, the information on the acceleration is needed for state feedback and can be calculated from eq.(1). For this, it is generally required to know all the inputs given to the system. However, in a real system, there are many cases where some of the inputs are unknown or inaccessible. For the unknown and inaccessible inputs, the observer was studied by Meditch and Hostetter and a 0-observer is selected for simplicity [11]. Thus, inaccessible load torque(T_L) is assumed to be an unknown constant. For a PMSM, the system equation for a disturbance torque observer can be expressed as follows :

$$\frac{dz}{dt} = Dz + Ew,\ y = \Omega = Cz \tag{16}$$

where

$$z = \begin{pmatrix} \Omega \\ T_L \end{pmatrix} = \begin{pmatrix} z_1 \\ z_2 \end{pmatrix},\ D = \begin{pmatrix} \frac{-F}{J} & \frac{-1}{J} \\ 0 & 0 \end{pmatrix},\ E = \begin{pmatrix} \frac{3P\Phi}{2J} \\ 0 \end{pmatrix},\ C = (1\ 0),\ w = i_q .$$

For this system, (D, C) is observable. The well-known asymptotic load torque observer can be designed as

$$\frac{d\hat{z}}{dt} = D\hat{z} + Ew + L(y - C\hat{z}) \tag{17}$$

where $\hat{z}$ is the observed value and $L = (l_1\ \ l_2)^T$ is the observer gain matrix.

III. Quasi-Linearized and Decoupled Model and Proposed Control Strategy

1. Quasi-Linearized and Decoupled Model

The actual nonlinear control input which employs the nominal parameter values and mechanical speed measured by a speed sensor is expressed as follows [7] :

$$\begin{pmatrix} v_d \\ v_q \end{pmatrix} = A_o^{-1}\left(-B_o + \begin{pmatrix} \nu'_1 \\ \nu'_2 \end{pmatrix}\right) \tag{18}$$

where ν'_1 and ν'_2 are the new control inputs and A_o, B_o are obtained from eqs.(7) and (8) using the nominal parameter values and measured speed. By Substituting eq.(18) into (6), a quasi-linearized and decoupled model can be obtained as follows :

$$\frac{di_d}{dt} = \frac{R_o - R}{L_d} i_d - P\frac{L_q}{L_d} i_q(\Omega_o - \Omega) + \nu'_1 = f_{n1}(x) + \nu'_1 \tag{19}$$

$$\frac{d^2\Omega}{dt^2} = -\frac{F}{J}\left(f_3 - f_{3o}\frac{\dot{\Phi}}{\Phi_o}\right) + P\frac{3\Phi}{2J}\left[\frac{R_o - R}{L_q} i_q + \frac{P}{L_q}(\Phi_o\Omega_o - \Phi\Omega) + P\frac{L_d}{L_q} i_d(\Omega_o - \Omega)\right] + \frac{\Phi}{\Phi_o}\frac{J_o}{J}\nu'_2 = f_{n2}(x) + b\nu'_2 \tag{20}$$

where the subscript "o" denotes the nominal parameter values and measured mechanical speed of motor. Unlike the linearized and decoupled model of eqs.(10) and (11), there are unwanted nonlinear terms $\hat{f}_{n2}(x)$ and $\hat{f}_{n1}(x)$, and control input gain b for the quasi-linearized and decoupled model of eqs.(19) and (20), which can degrade the control performances.

The unwanted nonlinear terms $f_{n1}(x)$ and $f_{n2}(x)$ are not exactly known but can be estimated as $\hat{f}_{n2}(x)$ and $\hat{f}_{n1}(x)$ and the estimation errors are bounded by some known functions $F_{n1}(x)$ and $F_{n2}(x)$. The control input gain b is also unknown but its bound can be deduced. Now, we consider the feedback linearization technique as a model-simplifying device for the robust control [9], and the new control inputs ν'_1 and ν'_2 are derived using a boundary layer integral sliding mode control technique to overcome the drawbacks of the conventional nonlinear control scheme.

2. Control Strategy for the Quasi-Linearized and Decoupled Model

Assume the bounds of parameter variations and speed measurement error as follows :

$$\begin{aligned} &R = \alpha R_o,\ \ \alpha_{\min}(=1.) \le \alpha \le \alpha_{\max}(=1.5) \\ &J = \beta J_o,\ \ \beta_{\min}(=1.) \le \beta \le \beta_{\max}(=4.) \\ &\Phi = \gamma\Phi_o,\ \ \gamma_{\min}(=0.8) \le \gamma \le \gamma_{\max}(=1.2) \\ &\Omega = \delta\Omega_o,\ \ \delta_{\min}(=1./1.05) \le \delta \le \delta_{\max}(1./0.95). \end{aligned} \tag{21}$$

Using eq.(21), the estimates $\hat{f}_{n1}(x)$ and $\hat{f}_{n2}(x)$, and the estimation error bounds $F_{n1}(x)$, $F_{n1}(x)$ of $f_{n1}(x)$, $f_{n2}(x)$ for the quasi-linearized and decoupled model can be obtained as follows :

$$\hat{f}_{n1} = \frac{1 - \alpha_{\max}}{L_d} R_o i_q - P\frac{L_q}{2L_d} i_q(2 - \delta_{\min} - \delta_{\max})\Omega_o \tag{22}$$

$$F_{n1} = \left|\frac{1 - \alpha_{\max}}{L_d} R_o i_q - P\frac{L_q}{2L_d} i_q(\delta_{\max} - \delta_{\min})\Omega_o\right| \tag{23}$$

$$\begin{aligned} \hat{f}_{n2} = \frac{1}{2}\Big[&\frac{3}{2}PFi_q\frac{\Phi_o}{J_o^2}\left(\frac{\gamma_{\max}}{\beta_{\min}} - \frac{\gamma_{\max}}{\beta_{\min}^2} + \frac{\gamma_{\max}}{\beta_{\min}} - \frac{\gamma_{\max}}{\beta_{\max}\beta_{\min}}\right) \\ &+ \frac{F^2\Omega_o}{J_o}\left(\frac{\delta_{\min}}{\beta_{\min}\beta_{\max}} - \frac{\gamma_{\max}}{\beta_{\min}} + \frac{\delta_{\max}}{\beta_{\min}^2} - \frac{\gamma_{\min}}{\beta_{\min}}\right) + \frac{F\hat{T}_L}{J_o^2}\left(\frac{1}{\beta_{\min}\beta_{\max}} - \frac{\gamma_{\max}}{\beta_{\min}}\right. \\ &\left. + \frac{1}{\beta_{\min}^2} - \frac{\gamma_{\min}}{\beta_{\min}}\right)\Big] + \frac{1}{2}\Big[P\frac{3\Phi_o}{2J_o}\Big[\frac{\gamma_{\max}}{\beta_{\min}}\frac{(1 - \alpha_{\max})}{L_q} R_o i_q \\ &+ \frac{\gamma_{\max}}{\beta_{\min}} P\frac{L_d}{L_q}(1 - \delta_{\max})\Omega_o i_d + \frac{\gamma_{\max}}{\beta_{\min}} P\frac{(1 - \gamma_{\max}\delta_{\max})}{L_q}\Phi_o\Omega_o \\ &+ \frac{\gamma_{\max}}{\beta_{\min}} P\frac{L_d}{L_q}(1 - \delta_{\min})\Omega_o i_d + \frac{\gamma_{\max}}{\beta_{\min}} P\frac{(1 - \gamma_{\min}\delta_{\min})}{L_q}\Phi_o\Omega_o\Big]\Big] \end{aligned} \tag{24}$$

$$F_{n2}=|\frac{1}{2}[\frac{3}{2}PFi_q\frac{\Phi_o}{J_o^2}(-\frac{\gamma_{max}}{\beta_{min}}+\frac{\gamma_{max}}{\beta_{min}^2}+\frac{\gamma_{max}}{\beta_{min}}-\frac{\gamma_{max}}{\beta_{max}\beta_{min}})$$
$$+\frac{F^2\Omega_o}{J_o}(-\frac{\delta_{min}}{\beta_{min}\beta_{max}}+\frac{\gamma_{max}}{\beta_{min}}+\frac{\delta_{max}}{\beta_{min}^2}-\frac{\gamma_{min}}{\beta_{min}})+\frac{F\hat{T}_L}{J_o^2}(-\frac{1}{\beta_{min}\beta_{max}}+\frac{\gamma_{max}}{\beta_{min}}$$
$$+\frac{1}{\beta_{min}^2}-\frac{\gamma_{min}}{\beta_{min}})]+\frac{1}{2}[P\frac{3\Phi_o}{2J_o}[-\frac{\gamma_{max}}{\beta_{min}}\frac{(1-\alpha_{max})}{L_q}R_oi_q$$
$$-\frac{\gamma_{max}}{\beta_{min}}P\frac{L_d}{L_q}(1-\delta_{max})\Omega_oi_d-\frac{\gamma_{max}}{\beta_{min}}P\frac{(1-\gamma_{max}\delta_{max})}{L_q}\Phi_o\Omega_o$$
$$+\frac{\gamma_{max}}{\beta_{min}}P\frac{L_d}{L_q}(1-\delta_{min})\Omega_oi_d+\frac{\gamma_{max}}{\beta_{min}}P\frac{(1-\gamma_{min}\delta_{min})}{L_q}\Phi_o\Omega_o]]|. \quad (25)$$

The bound on control input gain is

$$b_{min}(=\frac{\gamma_{min}}{\beta_{max}}=0.2)\le b\le b_{max}(=\frac{\gamma_{max}}{\beta_{min}}=1.2). \quad (26)$$

Using eqs.(22) through (26), the design problem of the sliding mode controller for the quasi-linearized and decoupled model of eqs.(19) and (20) is well introduced in a previous work [9]. The boundary layer integral sliding mode controller is considered to avoid the chattering phenomenon and the reaching phase problem [9, 12-13]. The sliding surface s_1 is chosen for the input-output decoupled form of eq.(19) [9, 14].

$$s_1=(\frac{d}{dt}+\lambda_1)\int_0^t e_1dt=e_1+\lambda_1\int_0^t e_1dt-e_1(0) \quad (27)$$

And the control law for ν'_1 is designed to guarantee $s_1\dot{s}_1<-\eta_1|s_1|$ as

$$\nu'_1=\hat{\nu}_1-k_1sat(\frac{s_1}{\phi_1}) \quad (28)$$

where $\hat{\nu}_1=-\hat{f}_{n1}-\lambda_1e_1$, $k_1=F_{n1}+\eta_1$, and $sat(\cdot)$ is the saturation function. Also, λ_1 and η_1 are the strictly positive constants. From eq.(27), it can be noted that $s_1=0$ from time $t=0$ and there is no reaching phase problem.

From the bound on control input gain b of eq.(26), the geometric mean b_m can be defined as

$$b_m=(b_{min}\,b_{max})^{1/2}=(\frac{\gamma_{min}\gamma_{max}}{\beta_{max}\beta_{min}})^{1/2}. \quad (29)$$

The bound on b can then be written in the form of

$$\Psi^{-1}\le\frac{b_m}{b}\le\Psi \quad (30)$$

where

$$\Psi=(\frac{b_{max}}{b_{min}})^{1/2}=(\frac{\gamma_{max}\beta_{max}}{\gamma_{min}\beta_{min}})^{1/2}.$$

The sliding surface s_2 is chosen for the input-output decoupled form of eq.(20) [9, 14].

$$s_2=\left(\frac{d}{dt}+\lambda_2\right)^2\int_0^t e_2dt=\frac{de_2}{dt}+2\lambda_2e_2+\lambda_2^2\int_0^t e_2dt-\frac{de_2}{dt}|_{t=0}-2\lambda_2e_2(0) \quad (31)$$

And the control law for ν'_2 is designed as shown in eq.(32) to guarantee $s_2\dot{s}_2<-\eta_2|s_2|$.

$$\nu'_2=b_m^{-1}(\hat{\nu}_2-k_2sat(\frac{s_2}{\phi_2})) \quad (32)$$

where $\hat{\nu}_2=-\hat{f}_{n2}-2\lambda_2\,de_2/dt-\lambda_2^2e_2$, $k_2=\Psi(F_{n2}+\eta_2)+(\Psi-1)|\hat{\nu}_2|$, and λ_2 and η_2 are strictly positive constants. From eq.(31), it can also be noted that $s_2=0$ from time $t=0$ and there is no reaching phase problem.

The bounds of uncertainties of the unwanted terms needed for the robust nonlinear control are obtained by deriving a quasi-linearized and decoupled model and the robustness is obtained by using these bounds to generate the control inputs which compensate the parameter uncertainties and speed measurement error. The overall scheme of the proposed robust nonlinear speed control system is shown in Fig. 2.

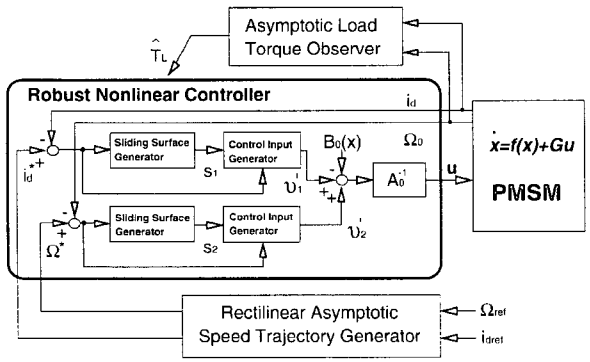

Fig. 2. Block diagram of the proposed robust nonlinear control scheme.

IV. Simulations and Experimental Results

1. System Configuration

The simulations and experimental works are carried out for the PMSM with the specifications as listed below.

$R_o=3\,ohm$, $L_d=L_q=7\,mH$, $\Phi_o=0.167\,Wb$,
$J_o=1.314\cdot10^{-4}Nmsec^2$, $F=2\cdot10^{-3}Nmsec$, $P=2$
rated speed $=3000\,RPM$, *rated power* $=400\,W$, *rated torque* $=1.274Nm$.

The configuration of the DSP-based experimental system is shown in Fig. 3. The main processor of the experimental system is a floating point Digital Signal Processor TMS320C30 with clock frequency of 32MHz [15-16]. The PMSM is driven by a three phase voltage source PWM inverter using an intelligent power module with a switching frequency of 7.8 kHz. The brushless resolver and resolver to digital converter are used to detect the absolute rotor position and speed of the PMSM. The resolution of detected position is selected as 12 bits. The phase currents are detected by the Hall-effect devices and the measured analogue signals are converted to digital values using the Analog to Digital converter with a 12 bit resolution. The PWM gate firing signals for the desired phase voltage commands are generated

by using the space vector modulation technique [17]. The sampling period of the control system is set as 128 μsec.

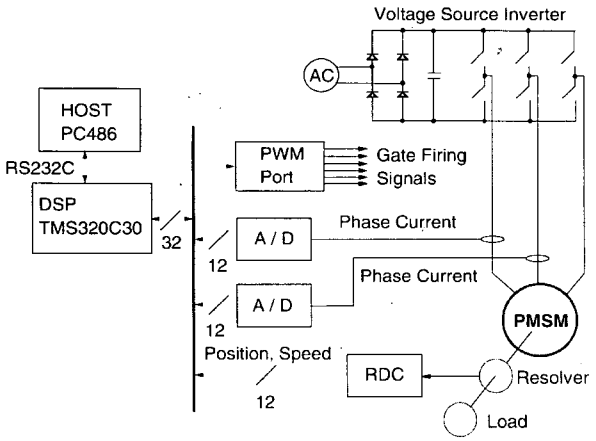

Fig. 3. Configuration of DSP-based experimental system.

To examine the performance of the proposed control scheme, the dynamic behavior of the control system is tested under the inertia or flux variations in the acceleration region with the acceleration time of 20 msec.

2. Simulation Results

To show the validity of the proposed control scheme, the computer simulations are carried out for the systems shown in Figs. 1 and 2 under various conditions. Fig. 1 shows the overall block diagram of the conventional nonlinear speed controller and Fig. 2 shows the proposed robust nonlinear speed controller. The design parameters ($K_{11}=2700$, $K_{21}=900$, and $K_{22}=810000$) used for the conventional nonlinear control scheme are selected to obtain nearly the same performances as those of the proposed control scheme when there are no parameter variations or disturbances. For the proposed robust nonlinear control scheme, the design parameters are selected as $\lambda_1=2700$, $\lambda_2=900$, $\eta_1=1$, $\eta_2=10$, $\phi_1=0.005$, and $\phi_2=5000$. It can be noted from eq.(31) that the sliding surface is a weighted sum of terms related to a tracking error and the large boundary layer thickness does not mean a large tracking error [9]. The observer gains used for the asymptotic observer are selected as $l_1=796.67$ and $l_2=-21.024$ to locate the double observer poles at -400 when there are no parameter variations. Figs. 4(a) and (b) show the speed response and quadrature axis current under no inertia variation($J=J_o$) for both control schemes. Figs. 5(a) and (b) show the same phenomena under the inertia variation of +200%($J=3J_o$). As shown in Figs. 4(a) and 5(a), the conventional nonlinear control scheme shows significant degradation in the transient response. Under the inertia variation of +200%, it shows the enhanced overshoot of 12% and prolonged settling time of 70msec. However, as shown in Figs. 4(b) and 5(b), the proposed robust nonlinear control

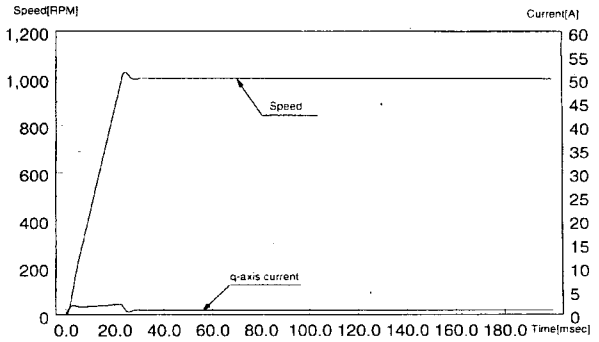

(a) Conventional control scheme

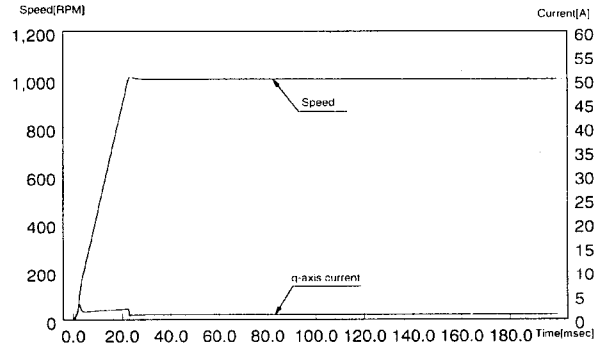

(b) Proposed control scheme

Fig. 4. Speed response and q-axis current under no inertia variation.

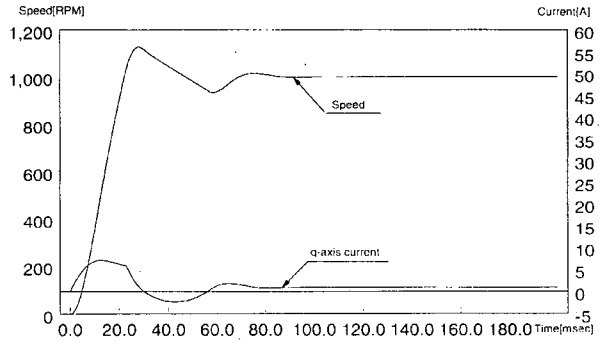

(a) Conventional control scheme

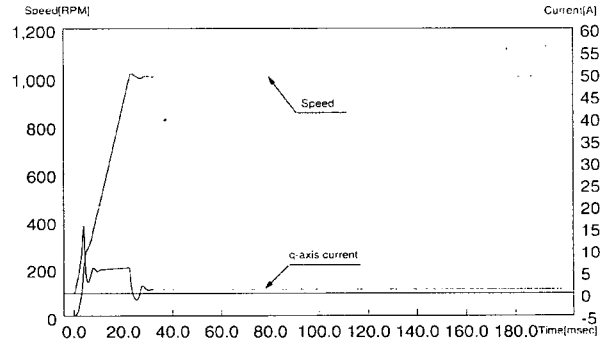

(b) Proposed control scheme

Fig. 5. Speed response and q-axis current under +200% inertia variation.

scheme shows a good performance without such a degradation. Fig. 6(a) shows the speed response and quadrature axis current with inertia variation of +50% only. And, Figs. 6(b) and (c) show the speed response and quadrature axis current with inertia variation of +50% and +10% flux variation for the conventional nonlinear control scheme and the proposed robust nonlinear control scheme, respectively. As shown in Fig. 6(a), for the inertia variation of +50% only, it shows overshoot of 6% and settling time of 30msec. On the other hand, as shown in Fig. 6(b) for the inertia variation of +50% and +10% flux variation it shows

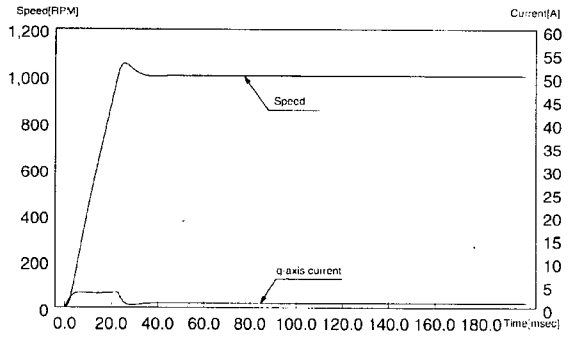

(a) Conventional control scheme under +50% inertia variation only

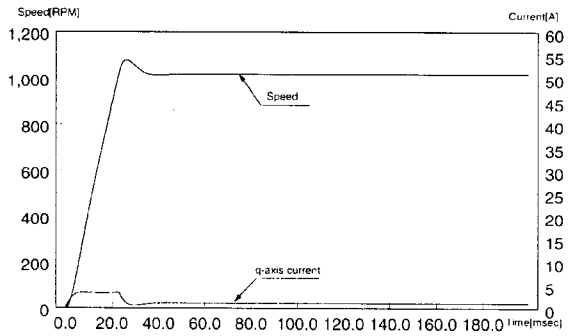

(b) Conventional control scheme under +50% inertia variation and 10% flux variation

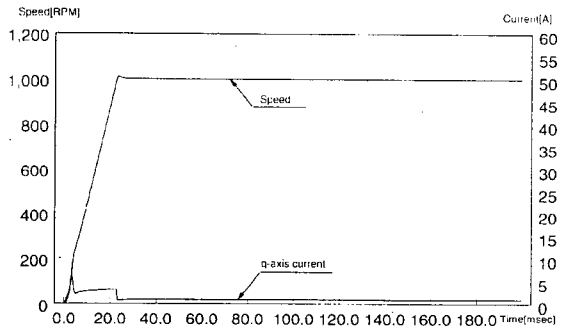

(c) Proposed control scheme under +200% inertia variation and +10% flux variation

Fig. 6. Speed response and q-axis current with inertia and(or) flux variations.

enhanced overshoot of 17% and prolonged settling time of 45msec. From Figs. 6(a) and (b), it can be noted that the additional degradation in the transient response is occurred due to flux variations. However, as shown in Fig. 6(c), the proposed robust nonlinear control scheme shows a good performance without such a degradation.

3. Experimental Results

The experimental works are carried out for the conventional and proposed control schemes. The same design parameters given in the previous section are used in both control schemes. The dynamic responses for both control schemes under the various conditions are shown in Figs. 7-9. As shown in Figs. 7(a) and 7(b), both control schemes provide a good dynamic response corresponding to the design specifications when there is no inertia variation($J=J_o$). However, when the inertial load is increased($J=3J_o$) in the conventional nonlinear control scheme, the overshoot and settling time are increased up to 12% and 50 msec as shown in Fig. 8(a). On the other hand, the proposed improved nonlinear control scheme provides the nearly same responses

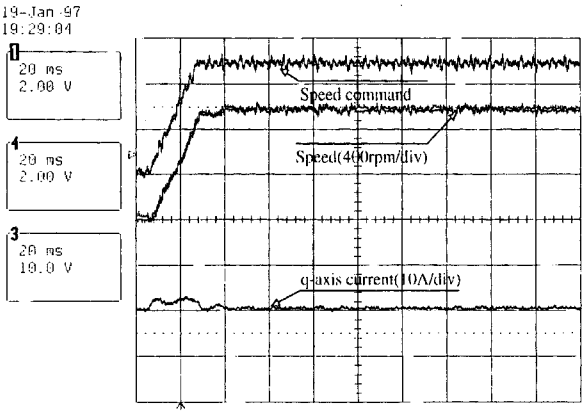

(a) Conventional control scheme

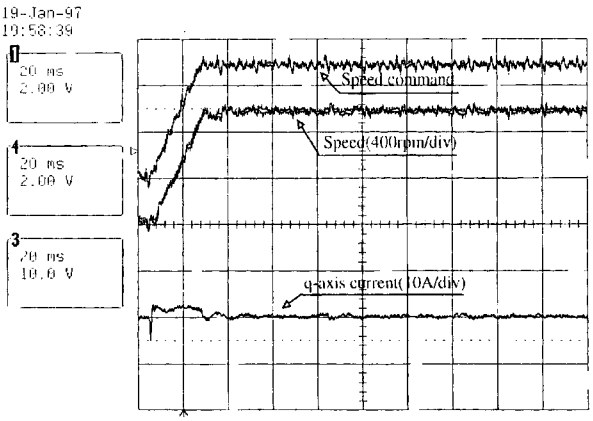

(b) Proposed control scheme

Fig. 7. Speed response and q-axis current under no inertia variation [experiments].

for both cases as shown in Figs. 7(b) and 8(b). As shown in Fig. 9(a), for the case of +50% inertia variation only, the conventional control scheme shows overshoot of 5% and settling time of 45msec. From Figs. 9(b) and 9(c), for the case of +50% inertia variation and +10% flux variation, the conventional control scheme shows increased overshoot of 10% and settling time of 50msec. However, the proposed control scheme also provides a good response. It can be observed from the experimental results in Figs. 7(b), 8(b) and 9(c) that there are no control chattering in the quadrature axis current by employing the boundary layers [9]. Even though some differences exist between simulations and experimental results mainly due to the unknown friction coefficient, and so on, it can be considered that the above simulations and experimental results well verify the validity of the proposed robust nonlinear control scheme.

Fig. 10 shows the values of sliding surfaces s_1 and s_2 for the proposed control scheme when there is an +200% inertia variation. It can be noted that the sliding surfaces are bounded within the boundary layers and these values are

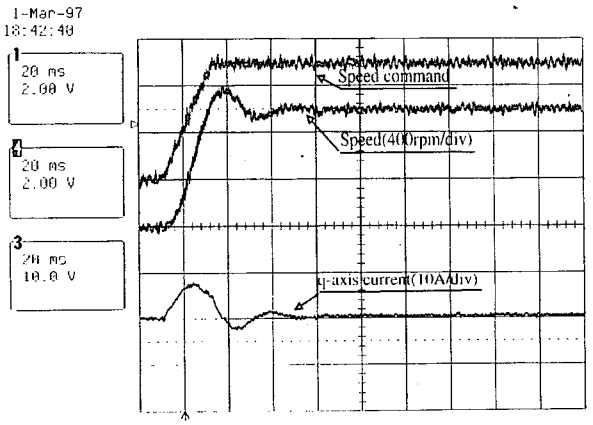

(a) Conventional control Scheme

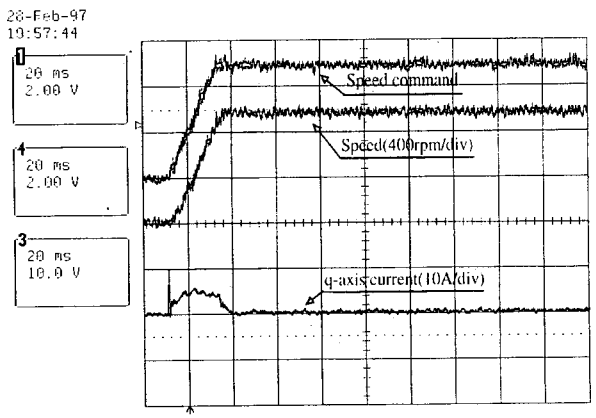

(b) Proposed control scheme

Fig. 8. Speed response and q-axis current under +200% inertia variation [experiments].

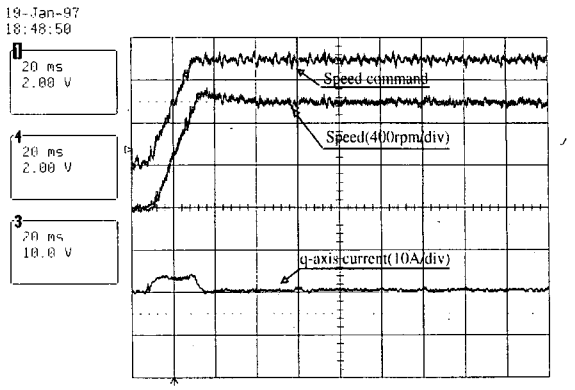

(a) Conventional control scheme under +50% inertia variation only

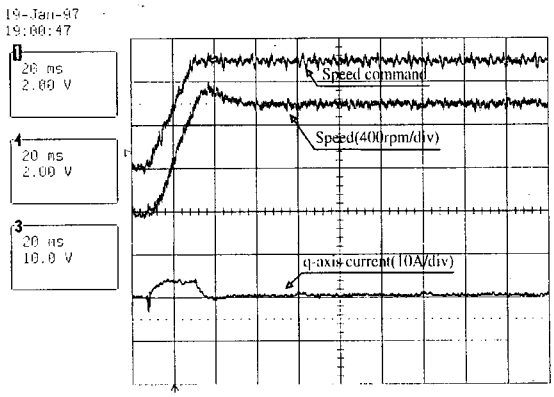

(b) Conventional control scheme under +200% inertia variation and 10% flux variation

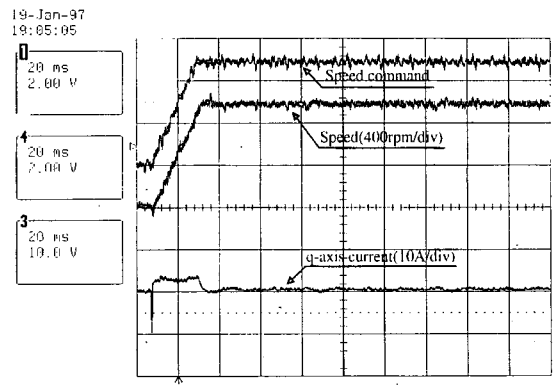

(c) Proposed control scheme and +200% inertia variation and +10% flux variation

Fig. 9. Speed response and q-axis current under inertia and(or) flux variations [experiments]

zeroes at the beginning of control actions. Therefore, it can be said that the sliding conditions are satisfied from the beginning of control actions without reaching phase problems.

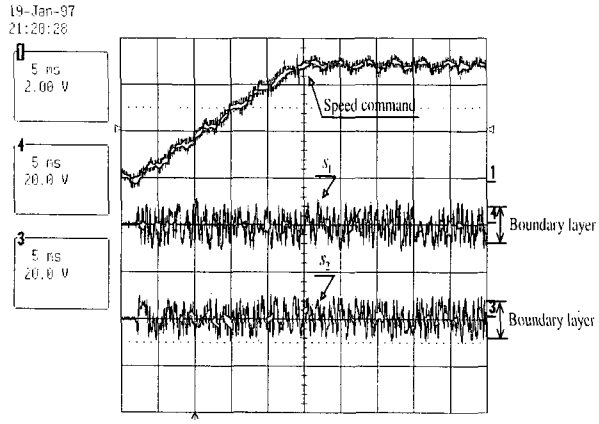

Fig. 10. Values of sliding surfaces s_1 and s_2 during speed transient under +200% inertia variation [experiment].

V. Conclusion

This paper proposes a robust nonlinear speed control scheme for a PMSM which guarantees the robustness in the presence of parameter variations and speed measurement error. The influence of parameter variations and speed measurement error on the nonlinear speed control of a PMSM is investigated and a quasi-linearized and decoupled model is derived. Based on this model, the design methods for the proposed control scheme have been given using the boundary layer integral sliding mode control technique. The bounds of uncertainties needed for the sliding mode control are deduced and the robustness is obtained by using these bounds to generate the control inputs which compensate the parameter uncertainties and disturbances. By introducing the boundary layer integral sliding mode technique, the chattering phenomenon and reaching phase problem can be avoided.

To show the validity of the proposed control scheme, the comparative simulations and experiments were carried out under various conditions. The distinctive results of this study can be summarized as follows. Compared with the conventional nonlinear control scheme, the proposed robust nonlinear control scheme provides good transient responses for the inertia variations and flux variations. For the proposed control scheme, the chattering phenomenon and reaching phase problem can be avoided by introducing boundary layer integral sliding mode technique. It can be said from these results that the proposed control scheme has the robustness against the unknown disturbances. Therefore, it can be expected that the proposed control scheme can be applied to the high performance applications such as the machine tools and robots.

References

[1] G. Champenois, P. Mollard, and J. P. Rognon, "Synchronous servo drive: a special application", *IEEE-IAS Conf. Rec.*, 1986, pp.182-189.

[2] M. Fadel and B. De Fornel, "Control laws of a synchronous machine fed by a PWM voltage source inverter", *EPE*, Aachen, RFA, Oct. 1989.

[3] W. Leonhard, *Control of electrical drives.* Springer Verlag, 1985.

[4] T. Rekioua, F. Meibody Tabar, J. P. Caron, and R. Le Doeuff, "Study and comparison of two different methods of current control of a permanent magnet synchronous motor", *Conf. Rec. IMACS-TC1*, Nancy, France, Vol.1, pp.157-163, 1990.

[5] B. Le Pioufle and J. P. Louis, "Influence of the dynamics of the mechanical speed of a synchronous servomotor on its torque regulation, proposal of a robust solution", *EPE*, Florence, Vol. 3, pp.412-417, 1991.

[6] J. J. Carroll Jr. and D. M. Dawson, "Integrator backstepping techniques for the tracking control of permanent magnet brush DC motors", *IEEE Trans. IA*, Vol. 31, no. 2, pp.248-255, Mar./April 1995.

[7] B. Le Pioufle, "Comparison of speed nonlinear control strategies for the synchronous servomotor", *Electric Machines and Power Systems*, Vol.21, pp.151-169, 1993.

[8] A. Isidori, *Nonlinear control systems: an introduction.* Springer-Verlag, 1985.

[9] J. J. Slotine and W. Li, *Applied nonlinear control.* Prentice-Hall, 1991.

[10] I. J. Nagrath, M. Gopal, *Control systems engineering.* John Wiley & Sons, 1982.

[11] J. Meditch and G. Hostetter, "Observers for systems with unknown and inaccessible inputs", *Int. J. Control*, Vol.19, no. 3, pp.473-480, 1974.

[12] T. L. Chern and Y. C. Wu, "Design of brushless DC position servo systems using integral variable structure approach", *IEE Proc.-B EPA*, Vol.140, no.1, pp.27-34, 1993.

[13] J. H. Lee, *Design of Integral-Augmented Optimal Variable Structure Controllers,* Ph.D. Dissertation, KAIST, 1995.

[14] J. Y. Hung, W. Gao, and J. C. Hung, "Variable structure control: A survey", *IEEE Trans. IE*, Vol.40, no.1, pp.2-22, 1993.

[15] TMS320C3X Users Guide, Texas Instruments Inc., 1990.

[16] TMS320C30 Assembly Language Tools Users Guide, Texas Instruments Inc., 1990.

[17] T. Kenjo, *Power Electronics for the Microprocessor Age.* Oxford University Press, 1990.

In-Cheol Baik was born in Seoul, korea on February 25, 1962. He received the B.S. degree in electronics from Konkuk University in 1984 and the M.S. and Ph.D. degrees in electrical engineering from the Korea Advanced Institute of Science and Technology (KAIST) in 1987 and 1998, respectively. He was a recipient of the University scholarship from Konkuk University during 1980-1982. He has been with the Living system research laboratory of LG Electronics Inc., Seoul from 1987. From February to May 1990, he took the Application Engineer course at SIEMENS Energy & Automation Training Center, Manchester, U.K. His research interests include rotating elcetrical machine drive systems, electric power conversion systems, and control engineering. Dr. Baik is a member of the Korean Institute of Power Electronics(KIPE) and KIEE.

Myung-Joong Youn was born in Seoul, Korea, on November 26, 1946. He received the B.S. degree from Seoul National University, Seoul, Korea, in 1970, and the M.S. and Ph.D. degrees in electrical engineering from the University of Missouri-Columbia in 1974 and 1978, respectively. He was with the Air-craft Equipment Division of General Electric Company at Erie, Pennsylvania, Since 1978, where he was as Individual Contributor on Aerospace Electrical Engineering. He has been with the Korea Advanced Institute of Science and Technology since 1983 where he is now a professor. His research activities are in the areas on power electronics and control which include the drive system, rotating electrical machine design, and high-performance switching regulators. Dr. Youn is a member of KIEE and KITE.

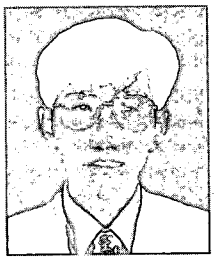

Kyeong-Hwa Kim was born in Seoul, Korea, on March 11, 1969. He received the B.S. degree in Electrical Engineering from Han-Yang University, Seoul, Korea, in 1991, and the M.S. degree in Electrical Engineering from Korea Advanced Institute of Science and Technology(KAIST), Taejon, Korea, in 1993. He is currently working toward the Ph. D. Degree in Electrical Engineering at KAIST. His research interests are in the areas on power electronics and control, which include machine drives and micropocessor based control applications.